JPE 15-6-17

http://dx.doi.org/10.6113/JPE.2015.15.6.1577
ISSN(Print): 1598-2092 / ISSN(Online): 2093-4718

Lyapunov Based Adaptive-Robust Control of the Non-Minimum phase DC–DC Converters Using Input–Output Linearization

Mahdi Salimi† and Adel Zakipour*

†,*Department of Electrical Engineering, Ardabil Branch, Islamic Azad University, Ardabil, Iran

Abstract

In this research, a combined adaptive-robust current controller is developed for non-minimum-phase DC–DC converters in a wide range of operations. In the proposed nonlinear controller, load resistance, input voltage and zero interval of the inductor current are estimated using developed adaptation rules and knowing the operating mode of the converter for the closed-loop control is not required; hence, a single controller can be employed for a wide load and line changes in discontinuous and continuous conduction operations. Using the TMS320F2810 digital signal processor, the experimental response of the proposed controller is presented in different operating points of the buck/boost converter. During transition between different modes of the converter, the developed controller has a better dynamic response compared with previously reported adaptive nonlinear approach. Moreover, output voltage steady-state error is zero in different conditions.

Key words: Adaptive control, Dynamic response, Lyapunov based control, Robust

I. INTRODUCTION

In spite of the nonlinear nature of power electronics systems, small-signal modeling and linear controllers are widely used in closed-loop control of the converters. However, approximated small signal models cannot describe the behavior of the nonlinear converter in different operating points. As generally known, during variation of the input voltage and load value in a wide range, application of the nonlinear closed-loop controller results in more stable response in DC–DC converters. For instance, design and development of the backstepping [1], exact feedback linearization [2], passivity-based [3] and sliding mode [4] approaches are reported in recent years.

Inductor current waveforms of a DC–DC converter in different operating modes are illustrated in Fig. 1. Modeling of the DC–DC converters in continuous mode is completely simple and for this reason, most of closed-loop controllers are designed in this operating mode [1]-[4]. Moreover, in high power applications, DC–DC converters have longer life time in continuous conduction [5]. In a discontinuous operation, a small inductor can be used and hence, dynamic response of the system will be absolutely fast. In low-power applications such as small battery chargers, a converter design in discontinuous operation is more economical [6]. Note that different closed-loop controllers are proposed for DC–DC converters in discontinuous operation [7], [8].

In some applications such as piezoelectric driver circuits, employing the DC–DC converter is required in both discontinuous and continuous modes. In addition, transition between different operating modes can improve the efficiency of the DC–DC converters [9]. As generally known, the model and behavior of the converters in continuous conduction mode is different from the discontinuous operation; for example, transition between operating modes can result in instability of the DC–DC regulators [10].

Generally, in a wide range of operation, determining the operating mode of power converter for closed-loop control of the system is required. In fact, two different controllers are usually designed for different operating modes, and a suitable controller is selected by online measurement of the inductor current [11]. In this approach, switching between different controllers can clearly deteriorate fast dynamic response of

Manuscript received Mar. 6, 2015; accepted May 18, 2015
Recommended for publication by Associate Editor Se-Kyo Chung.
†Corresponding Author: m.salimi@iauardabil.ac.ir
Tel: +98-914-152-8983, Department of Engineering, Ardabil Branch, Islamic Azad University, Ardabil, Iran
*Department of Electrical Engineering, Ardabil Branch, Islamic Azad University, Ardabil, Iran

© 2015 KIPE

the converter. Hence, development of a single controller for both modes can significantly improve systems dynamic response.

In adaptive controllers, continuously adjusting the gains of the control loop is possible. Hence, the dynamic response of the system can be improved in the presence of uncertain parameters. It is possible to implement these controllers using standard digital signal processors. For example, in [10], application of the adaptive controller is reported for both modes of the operation in DC–DC buck converters. However, the controller of [10] is designed using a small-signal model. Hence, the controller cannot be applied in a wide range of operation. Moreover, according to non-minimum phase nature of the boost status, this controller cannot be used directly in DC–DC buck/boost converters. Although adaptive nonlinear controllers are designed for non-minimum phase DC–DC converters in discontinuous and continuous operations [12], [13], the applications of a single controller for both modes are not reported yet.

On the other hand, application of the sliding mode controller in closed-loop regulation of the DC–DC converters is completely reasonable because of inherent robustness to load and input voltage changes, ease of implementation, and fast dynamic response. The main drawbacks of this controller are variation of the switching frequency and presence of steady-state error that can be cancelled by using equivalent control approach and adding integral term into sliding surface.

To benefit from the advantages of the adaptive and sliding mode controllers, combining these controllers is possible. For example, in [14], an adaptive sliding mode controller is proposed for output voltage regulation of the DC–DC boost converter that is able to estimate variations of the input voltage and load resistance. However, the controller of [14] is designed only for a continuous mode of operation; hence, the stability of the proposed method cannot be guaranteed in a discontinuous operation and during transition between different modes. In addition, in [15], an adaptive robust controller is reported for DC–DC buck converter. However, a controller design is formulated for a continuous conduction mode, and the response of the system is evaluated only by a computer-based simulations. Moreover, in non-minimum phase DC–DC converters, directly using the controller of [15] is impossible.

In [16], an adaptive nonlinear approach is developed for closed-loop control of the DC–DC buck/boost converters. The proposed controller in [16] can be applied in both discontinuous and continuous conduction of the inductor current. However, the controller gain must be adjusted during the transition of the converter between different modes. In fact, two different controllers are required in a wide range of operations in [16]. Hence, the necessity for controller selection in different modes deteriorates dynamic the response of the system. Moreover, the response of the adaptive controllers depends on the accuracy of the system model that is used in the design process. In other words, if any unmolded dynamics exists in the system model, the response of the adaptive controller may be adversely affected. To increase the model accuracy in [16], the effect of the inductor equivalent series resistance is considered during the development of the controller. Considering all parasitic elements (such as the equivalent series resistance of the power switch, diode, and capacitor) in the converter model and their estimation by adaptive controller obviously increase the complexity of the system; hence, its application in the practical regulators will be difficult. On the other hand, such problem is not reported in robust controllers. Therefore, a combination of robust controllers with adaptive nonlinear approaches is completely desirable in DC–DC converters.

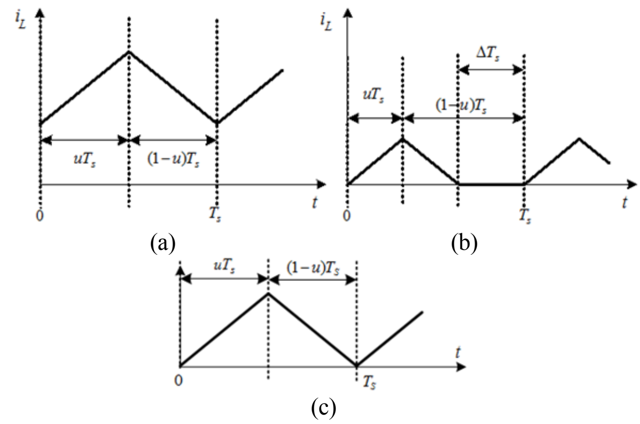

Fig. 1. (a) Inductor current waveform in continuous, (b) discontinuous. (c) Boundary conduction modes of operation.

As shown in Fig. 1, in addition to input voltage and load resistance, zero interval of the inductor current (Δ) is also an uncertain parameter. In continuous conduction mode, the value of Δ is equal to zero; in discontinuous operation, its value is a function of load resistance, switching frequency, and inductor value. As a result, the same model can be used to describe DC–DC converters in both operating modes by estimation of Δ. According to this idea, a combined adaptive-robust controller for both operating modes of the DC–DC buck/boost converter is proposed in this paper. Estimating the load resistance, input voltage and Δ using a developed nonlinear controller in a wide range of operation is possible.

The paper is organized as follows. The averaged state space model of the DC–DC buck/boost converter is formulated in Section II. Then, the proposed adaptive robust controller is applied to the DC–DC buck/boost converter and controller law and parameter estimation rules are derived in Section III. Finally, experimental response of the designed controller is presented in a wide range of operation, particularly during transition between different modes, in Section IV. As will be shown later, the proposed controller has better dynamic response compared to adaptive the nonlinear approach [16].

Moreover, the controller is completely stable in different modes with zero steady-state error.

II. Averaged State-Space Modeling of the DC–DC Buck/Boost Converter in Discontinuous and Continuous Conduction Modes

In Fig. 1, the inductor current waveform is illustrated in both operating modes. If $\Delta = 0$ is replaced in discontinuous model of the converter, obtaining continuous behavior of the system is possible. In fact, the converter model in the discontinuous operation covers the continuous model. Hence, the converter model in the discontinuous operation is used for the controller design. In the proposed controller, uncertain parameters of the model including Δ is estimated. Circuit topology of the standard DC–DC buck/boost converter is shown in Fig. 2.

During the ON state of the controlled switch, the diode is OFF. In this interval, the state-space model of the converter can be written as follows. In these equations, $\boldsymbol{X} = [x_1 \ \ x_2]^T$ is the state vector of the model.

$$\dot{\boldsymbol{X}} = \boldsymbol{A}_{on}\boldsymbol{X} + \boldsymbol{B}_{on}\ ;\ \boldsymbol{A}_{on} = \begin{bmatrix} 0 & 0 \\ 0 & -\frac{1}{RC} \end{bmatrix}, \boldsymbol{B}_{on} = \begin{bmatrix} \frac{V_{in}}{L} \\ 0 \end{bmatrix}. \quad (1)$$

When the controlled switch is turned off, the converter diode will be turned on. Hence,

$$\dot{\boldsymbol{X}} = \boldsymbol{A}_{off}\boldsymbol{X} + \boldsymbol{B}_{off};\ \ \boldsymbol{A}_{off} = \begin{bmatrix} 0 & -\frac{1}{L} \\ \frac{1}{C} & -\frac{1}{RC} \end{bmatrix}, \boldsymbol{B}_{off} = \begin{bmatrix} 0 \\ 0 \end{bmatrix}. \quad (2)$$

By continuing the inductor current reduction, a portion of the switching period in the discontinuous mode can become zero. In this case, the required energy of the load is supplied by the output capacitor, and the model of the system is

$$\dot{\boldsymbol{X}} = \boldsymbol{A}_{\Delta}\boldsymbol{X} + \boldsymbol{B}_{\Delta};\ \boldsymbol{A}_{\Delta} = \begin{bmatrix} 0 & 0 \\ 0 & -\frac{1}{RC} \end{bmatrix}; \boldsymbol{B}_{\Delta} = \begin{bmatrix} 0 \\ 0 \end{bmatrix}. \quad (3)$$

On the basis of the averaging technique in modeling of the power electronics converters, combining Equs. (1)–(3) is possible, and the following averaged state-space model can be obtained:

$$\dot{x}_1 = -\frac{1}{L}(1-u)x_2 + \rho_1 x_2 + \rho_2 u \quad (4)$$

$$\dot{x}_2 = \frac{1}{C}(1-u)x_1 + \rho_3 x_1 + \rho_4 x_2 \quad (5)$$

and

$$\rho_1 = \frac{\Delta}{L};\ \rho_2 = \frac{V_{in}}{L}\ ;\ \rho_3 = -\frac{\Delta}{C};\ \rho_4 = -\frac{1}{RC} \quad . \quad (6)$$

In these equations, ρ_i is the ith uncertain parameter where $i = 1\ to\ 4$. Furthermore, u is the duty cycle of the controlled switch.

III. Adaptive-Robust Controller Design

On the basis of the nonlinear behavior of the DC–DC buck/boost converter and the existence of several uncertain parameters in the model, in this paper, Lyapunov based adaptive controller is selected for controller design.

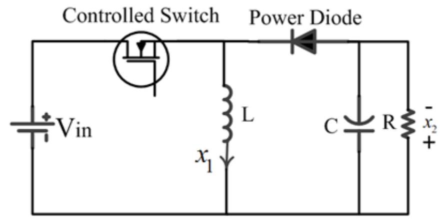

Fig. 2. DC–DC buck/boost converter.

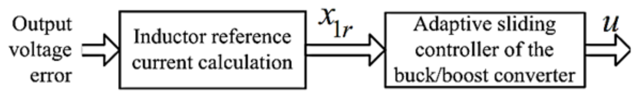

Fig. 3. Block diagram of the proposed double-loop controller.

To improve the robustness of the proposed controller against unmodelled dynamics, the sliding-mode controller is combined with an adaptive nonlinear approach. The block diagram of the developed controller is shown in Fig. 3. Inductor current is controlled in an inner loop using a developed adaptive-robust nonlinear controller. In addition, proportional–integral-based controller is employed in the outer loop that generates reference current of the inductor. The application of the double-loop structure in DC–DC converters enjoys the following advantages:

1. In adaptive and robust-based control of the DC–DC converters, the output voltage error is usually not zero. However, the PI controller in the outer loop eliminates the steady-state error.
2. During direct control of the output voltage, most of the DC–DC converters behave as non-minimum phase systems. Hence, indirect control of the output voltage using double-loop control improves stability of the system.

Adaptive-robust controller design: On the basis of the inductor current error ($e_1 = x_1 - x_{1r}$), the time-derivative can be written as follows:

$$\dot{e}_1 = \widehat{\mathbf{P}}^{\mathrm{T}}\mathbf{M}_1 - \frac{1}{L}(1-u)x_2 - \dot{x}_{1r} + \left(\mathbf{P} - \widehat{\mathbf{P}}\right)^{\mathrm{T}}\mathbf{M}_1 \quad (7)$$

where $\mathbf{P}^{\mathrm{T}} = (\rho_1\ \ \rho_2\ \rho_3\ \rho_4)$ and ${\mathbf{M}_1}^{\mathrm{T}} = (x_2\ u\ \ 0\ \ 0)$. In this step, $V_1 = 0.5{e_1}^2 + (\mathbf{P} - \widehat{\mathbf{P}})^{\mathrm{T}}\mathbf{\Gamma}^{-1}(\mathbf{P} - \widehat{\mathbf{P}})$ is considered as the first Lyapunov function. $\mathbf{\Gamma}$ is a 4×4 diagonal matrix with positive elements, which determines weights of the estimated parameters. The time derivative of the first Lyapunov function can be easily written as $\dot{V}_1 = e_1\dot{e}_1 + (\mathbf{P} - \widehat{\mathbf{P}})^{\mathrm{T}}\mathbf{\Gamma}^{-1}(-\dot{\widehat{\mathbf{P}}})$. Using equation (7), $\dot{V}_1$ can be re-written as follows:

$$\dot{V}_1 = e_1(\widehat{\mathbf{P}}^{\mathrm{T}}\mathbf{M}_1 - \frac{1}{L}(1-u)x_2 - \dot{x}_{1r}) + \left(\mathbf{P} - \widehat{\mathbf{P}}\right)^{\mathrm{T}}\mathbf{\Gamma}^{-1}(-\dot{\widehat{\mathbf{P}}} + \mathbf{\Gamma}e_1\mathbf{M}_1) \quad (8)$$

On the basis of $\left(\widehat{\mathbf{P}}^{\mathrm{T}}\mathbf{M}_1 - \frac{1}{L}(1-u)x_2 - \dot{x}_{1r}\right) = -k_1e_1$ and $(-\dot{\widehat{\mathbf{P}}} + \boldsymbol{\Gamma}e_1\mathbf{M}_1) = \mathbf{0}$, then using Equ. (8), $\dot{V}_1 = -k_1{e_1}^2$ will be obtained, which is a negative semi-definite function and results in asymptotical stability of the control system. In these equations, k_1 is a positive scalar. Because $\widehat{\mathbf{P}}^{\mathrm{T}}\mathbf{M}_1 - \frac{1}{L}(1-u)x_2 - \dot{x}_{1r}$ and $-k_1e_1$ are not necessarily equal, their difference is defined as the second error variable, i.e.,

$$e_2 = \hat{\rho}_1x_2 + \hat{\rho}_2\,u - \frac{1}{L}(1-u)x_2 - \dot{x}_{1r} + k_1e_1. \quad (9)$$

By combining Equs. (7) and (9), the following equation can be obtained:

$$\dot{e}_1 = -k_1e_1 + e_2 + \left(\mathbf{P} - \widehat{\mathbf{P}}\right)^{\mathrm{T}}\mathbf{M}_1. \quad (10)$$

Using Equs. (5), (7), and (9), the time derivative of the second error variable can be written as

$$\dot{e}_2 = A + \widehat{\mathbf{P}}^{\mathrm{T}}\mathbf{M}_2 + (\mathbf{P} - \widehat{\mathbf{P}})^{\mathrm{T}}\mathbf{M}_2 \quad (11)$$

where

$${\mathbf{M}_2}^{\mathrm{T}} = \begin{bmatrix} k_1x_2 \\ k_1u \\ x_1(\,\hat{\rho}_1 - \frac{1}{L}(1-u)) \\ x_2(\,\hat{\rho}_1 - \frac{1}{L}(1-u)) \end{bmatrix} \quad (12)$$

and

$$A = \dot{\hat{\rho}}_1x_2 + \frac{1}{L}(\dot{u})x_2 + \dot{\hat{\rho}}_2u + \hat{\rho}_1\frac{1}{C}(1-u)x_1 + \dot{\hat{\rho}}_2\,\dot{u} - \frac{1}{LC}(1-u)^2x_1 - \ddot{x}_{1r} + -k_1\frac{1}{L}(1-u)x_2 - k_1\dot{x}_{1r}. \quad (13)$$

In this step, the second Lyapunov function is assumed as $V_2 = 0.5{e_1}^2 + 0.5\mathrm{S}^2 + (\mathbf{P} - \widehat{\mathbf{P}})^{\mathrm{T}}\boldsymbol{\Gamma}^{-1}(\mathbf{P} - \widehat{\mathbf{P}})$, where $\mathrm{S} = \mathrm{c}_1e_1 + e_2$ is a sliding surface of the robust controller. $\dot{V}_2 = e_1\dot{e}_1 + S\dot{S} + (\mathbf{P} - \widehat{\mathbf{P}})^{\mathrm{T}}\boldsymbol{\Gamma}^{-1}(-\dot{\widehat{\mathbf{P}}})$ is clearly a derivative of the second Lyapunov function. To investigate systems stability, the derivative of sliding surface $\dot{\mathrm{S}} = \mathrm{c}_1\dot{e}_1 + \dot{e}_2$ can be calculated using Equs. (10) and (11), i.e.,

$$\dot{\mathrm{S}} = \mathrm{c}_1(-k_1e_1 + e_2) + A + \widehat{\mathbf{P}}^{\mathrm{T}}\mathbf{M}_2 + \left(\mathbf{P} - \widehat{\mathbf{P}}\right)^{\mathrm{T}}(\mathbf{M}_2 + \mathrm{c}_1\mathbf{M}_1). \quad (14)$$

According to Equ. (14), the time derivative of the second Lyapunov function can be written as

$$\dot{V}_2 = -k_1{e_1}^2 + e_1e_2 - k_1{\mathrm{c}_1}^2{e_1}^2 - k_1\mathrm{c}_1e_1e_2 + (e_2 + \mathrm{c}_1e_1)(A + \mathrm{c}_1e_2) + \left(\mathbf{P} - \widehat{\mathbf{P}}\right)^{\mathrm{T}}\boldsymbol{\Gamma}^{-1}[-\dot{\widehat{\mathbf{P}}} + \boldsymbol{\Gamma}e_1\mathbf{M}_1 + \boldsymbol{\Gamma}(\mathrm{c}_1e_1 + e_2)[2\mathbf{M}_2 + \mathrm{c}_1\mathbf{M}_1]].$$

Assuming that $A + \mathrm{c}_1e_2 = -b(S + Wsgn(S))$ and $-\dot{\widehat{\mathbf{P}}} + \boldsymbol{\Gamma}e_1\mathbf{M}_1 + \boldsymbol{\Gamma}(\mathrm{c}_1e_1 + e_2)[2\mathbf{M}_2 + \mathrm{c}_1\mathbf{M}_1] = \mathbf{0}$, then

$$\dot{V}_2 = -k_{e1}{e_1}^2 - k_{e12}e_1e_2 - bS^2 - bW|S|$$

where $-k_1 - k_1{\mathrm{c}_1}^2 = -k_{e1}$ and $-k_1\mathrm{c}_1 + 1 = -k_{e12}$. Showing that if $\mathrm{c}_1(k_1 + 2\mathrm{b}) < (2\sqrt{\mathrm{b}({\mathrm{c}_1}^2(k_1 + \mathrm{b}) + k_1)} + 1)$ is satisfied is completely straightforward. $\dot{V}_2$ will be a negative semi-definite function that guarantees asymptotical stability of the whole control system; for instance, the condition is clearly satisfied for $k_1 = \mathrm{c}_1 = \mathrm{b} = 1$.

Based on $A + \mathrm{c}_1e_2 = -b(S + Wsgn(S))$ and $-\dot{\widehat{\mathbf{P}}} + \boldsymbol{\Gamma}e_1\mathbf{M}_1 + \boldsymbol{\Gamma}\mathrm{S}[2\mathbf{M}_2 + \mathrm{c}_1\mathbf{M}_1] = \mathbf{0}$, the controller and parameter estimation rules can be obtained as follows:

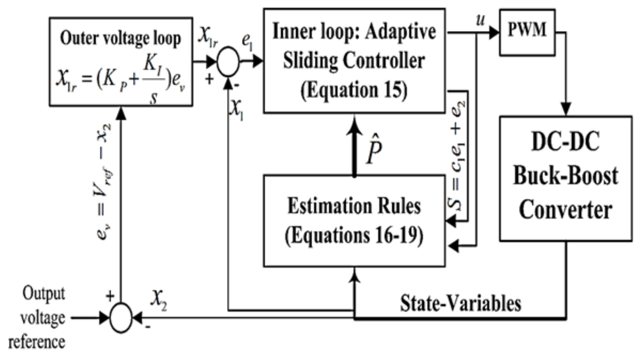

Fig. 4. Proposed adaptive-robust controller.

TABLE I
CIRCUIT PARAMETERS OF THE DC–DC BUCK/BOOST CONVERTER

Input voltage	12 V
Converter inductor	550 µH
Output capacitor	330 µF
Load resistance	200 Ω
Switching frequency	9.25 kHz
Sampling frequency	130 kHz

$$\dot{u} = \frac{1}{-\left(\frac{1}{L}x_2 + \hat{\rho}_2\right)}\Big\{[\dot{\hat{\rho}}_1 - k_1\frac{1}{L}(1-u)]x_2 + [\hat{\rho}_1\frac{1}{C}(1-u) - \frac{1}{LC}(1-u)^2]x_1 + \dot{\hat{\rho}}_2u - \ddot{x}_{1r} - k_1\dot{x}_{1r} + \mathrm{c}_1e_2 + b(S + Wsgn(S))\Big\} \quad (15)$$

$$\dot{\hat{\rho}}_1 = \gamma_{11}[2Sk_1x_2 + \mathrm{c}_1Sx_2 + e_1x_2] \quad (16)$$

$$\dot{\hat{\rho}}_2 = \gamma_{22}[2Sk_1u + \mathrm{c}_1Su + e_1u] \quad (17)$$

$$\dot{\hat{\rho}}_3 = \gamma_{33}[2Sx_1(\,\hat{\rho}_1 - \frac{1}{L}(1-u))] \quad (18)$$

and

$$\dot{\hat{\rho}}_4 = \gamma_{44}[\,2Sx_2(\,\hat{\rho}_1 - \frac{1}{L}(1-u))]. \quad (19)$$

IV. SIMULATION AND EXPERIMENTAL RESULTS

To evaluate the effectiveness of the proposed approach, the DC–DC buck/boost converter is implemented based on developed control law [Equ. (15)] and parameter adaptation rules [Equs. (16)-(19)]. The circuit parameters of the implemented DC–DC buck/boost converter are listed in Table I [16]. To analyze the response of the proposed controller to step changes in input voltage and load value, different power switches are used in the circuit topology of the converter. The state variables of the system are measured using isolated current and voltage sensors.

A Hall Effect current sensor is employed for inductor current sensing and IL300 integrated circuit for output voltage measurement. The state variables are converted to digital signals using 12-bit A/D circuits. Finally, the designed controller is implemented in TMS320F2810 digital signal processor according to the block diagram that is shown in Fig. 4. Moreover, some simulations are presented using MATLAB/Simulink toolbox.

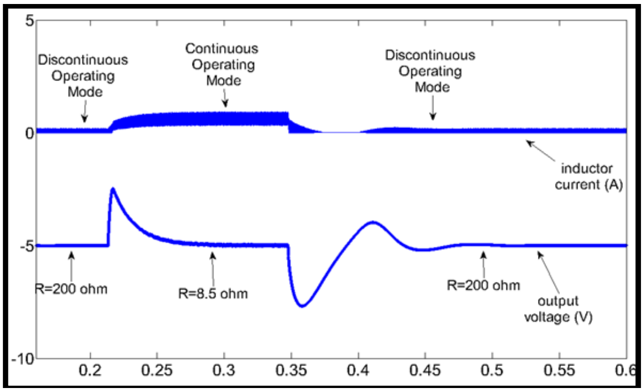

(a) Simulation.

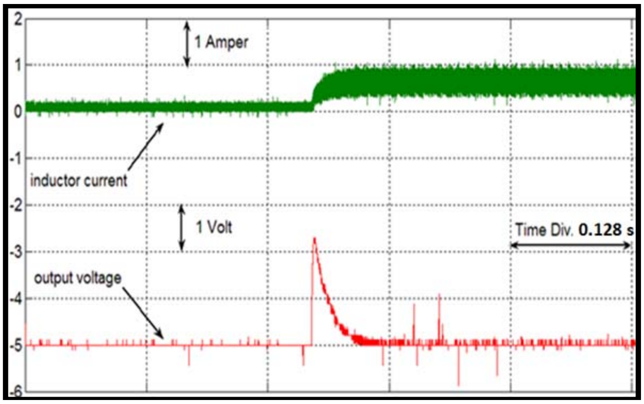

(b) Experimental.

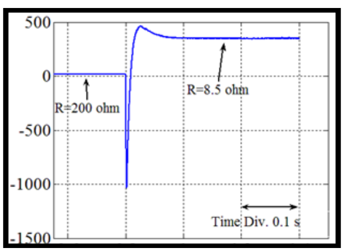

(c) Estimation of the $-\hat{\rho}_4 = \frac{1}{RC}$.

Fig. 5. Dynamic response of the proposed converter during transition from discontinuous conduction mode into continuous operation.

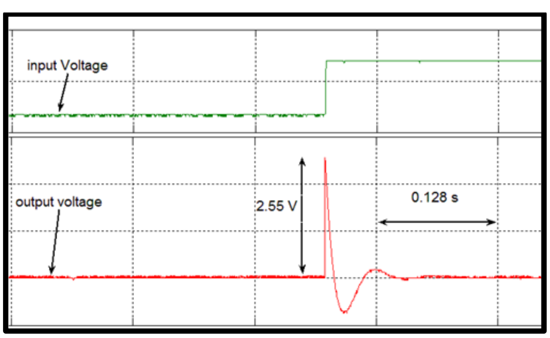

Fig. 6. Dynamic response of the proposed controller during step changes of the input voltage, load resistance, and capacitor (experimental).

Although separately testing the controller response in discontinuous or continuous conduction modes is possible, the capability of the proposed controller in both operating modes must be considered. The response is illustrated during transition from discontinuous into continuous mode in Fig. 5. In this test, load resistance is stepped between 200 Ωin discontinuous mode and 8.5 Ωin continuous operation. In spite of heavy fluctuations in load value and change of the system model, the developed adaptive-robust controller is stable with zero steady-state error. In the proposed controller, determining the converter operating mode is not required, and a single controller is employed in the whole operating range of the system. In Fig. 5, output voltage reference is -5 V. In this test, the estimation of the $-\hat{\rho}_4 = \frac{1}{RC}$ is illustrated in Fig. 5(c).

The dynamic response of the controller during variations of the input voltage, output resistance, and capacitor (all at the same time) is shown in Fig. 6. The converter parameters are stepped from nominal values in Table I to $R = 100\ \Omega$, $C = 660\ \mu\text{F}$, and $V_{in} = 17$ V. The output voltage reference value is -5 V, and the converter is in discontinuous operation. The proposed controller is obviously completely stable in different operating points. It should be noted that the main reason for the sudden voltage drop in Fig. 6 is the addition of a second capacitor with no charge in parallel with primary one. In fact, the initial charge of the first capacitor is shared with another capacitor, and hence, output voltage is reduced to half of the initial value. However, the proposed controller is clearly able to regulate and stabilize the output voltage of the converter. Moreover, if the output capacitor is kept constant during this test, sudden voltage change will not be present in the output voltage. For instance, in Fig. 7, the converter parameters are stepped from $R = 200\ \Omega$ and $V_{in} = 12$ V to $R = 100\ \Omega$ and $V_{in} = 17$ V.
The output voltage reference is assumed to be -5 V and that the converter operates in discontinuous mode.
Furthermore, in Fig. 8, the simulated response of the controller to step changes of the input voltage is shown from the start-up moment. First, the input voltage of the converter is stepped from +12 V to +17 V; then, after a few moments, it is stepped from +17 V to 22 V. The proposed controller is obviously completely robust to input voltage changes. Finally, the response of the proposed controller to reference voltage changes is illustrated in Fig. 9.

Based on the nominal values of the converter in Table I, reference voltage is stepped from -5 V to -15 V. In this test, the input voltage is +12 V; hence, the converter characteristic is changed from buck into boost operation. In spite of large variations in the output voltage, the proposed controller is clearly able to track the references with zero steady-state error and acceptable dynamic response. To evaluate the effectiveness of the designed controller in more detail, the dynamic response of the proposed Lyapunov based

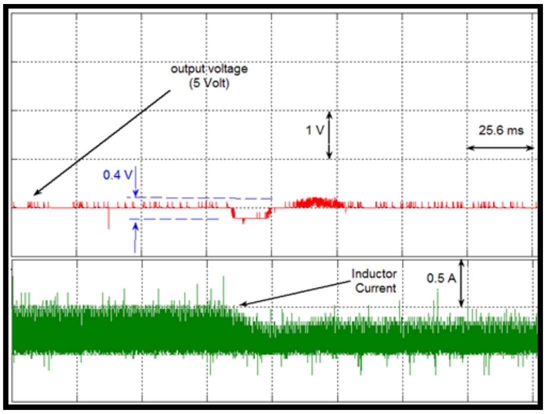

Fig. 7. Dynamic response of the proposed controller during step changes of the input voltage and load value (experimental).

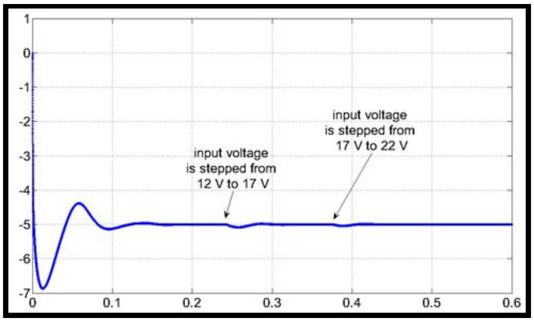

Fig. 8. Response of the proposed controller to step changes of the input voltage (simulation).

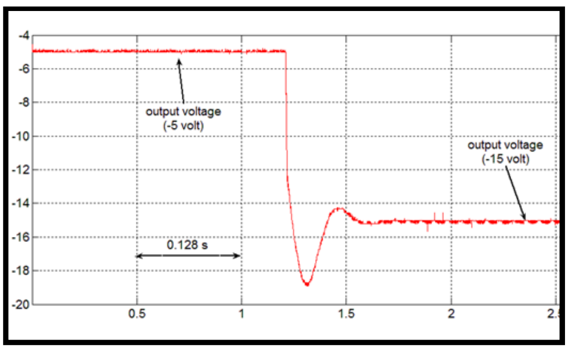

Fig. 9. Dynamic response of the proposed controller to step changes of the reference voltage (experimental).

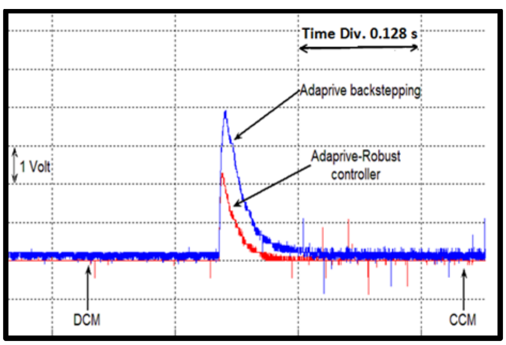

Fig. 10. Dynamic response of (red) the proposed controller in comparison with (blue) the adaptive nonlinear controller [16]*. (experimental).

adaptive-robust controller is compared with adaptive nonlinear controller of [16] during transition from discontinuous operation into continuous mode. In fact, considering similar conditions with the first test in Fig. 5, the dynamic response of the previously reported adaptive controller [16] is presented in Fig. 10 in comparison with the proposed adaptive-robust controller. The designed adaptive robust controller clearly has a better dynamic response with zero steady-state error.

V. CONCLUSION

In this paper, a Lyapunov based adaptive-robust controller is proposed for output voltage regulation of the non-minimum phase DC–DC buck/boost converter in discontinuous and continuous operations. The controller is able to estimate load resistance, input voltage, and zero portion of the inductor current using developed adaptation rules. Hence, a single controller can be applied in a wide range of the operation, and determining the operating mode of the converter is not required. The developed controller is robust with respect to unmodelled dynamics; therefore, the controller is not required to consider parasitic elements of the converter during state-space modeling. To evaluate the accuracy of the developed controller, DC–DC buck/boost converter is implemented using TMS320F2810 digital signal processor. Experimental results prove that the controller is stable in a wide range of load and line changes. Furthermore, the proposed adaptive-robust controller has better dynamic response compared with the adaptive nonlinear controller and the output voltage steady-state error is zero.

ACKNOWLEDGMENT

This research was supported by the Islamic Azad University, Ardabil Branch under a Research Grant.

REFERENCES

[1] H. El-Fadil, F. Giri, O. ElMagueri, and F. Z.Chaoui, “Control of DC–DC power converters in the presence of coil magnetic saturation,” *Control Engineering Practice* 17, pp. 849-862, 2009.

[2] H. Zheng and D. Shuai, “Nonlinear control of Boost converter by state feedback exact linearization,” *Control and Decision Conference (CCDC)*, 2012 24th Chinese, pp. 3502-3506, 2012.

[3] J. Zeng, Z. Zhang, and W. Qiao, “An interconnection and damping assignment passivity-based controller for a DC–DC boost converter with a constant power load,” *IEEE Trans. Ind. Appl.*, Vol. 50, No. 4, pp. 2314-2322, Jul./Aug. 2014.

[4] Y. Hey, W. Xu, and Y. Cheng, “A novel scheme for sliding-mode control of DC-DC converters with a constant frequency based on the averaging model,” *Journal of Power Electronics*, Vol. 10, No. 1, pp. 1-8, Jan. 2010.

[5] H. M. Pang and B. M. H. Pong, “Design-oriented model and critical inductance method for long life isolated power converters,” *IET Power Electronics,* Vol. 6, No. 9, pp. 1862-1871, Nov. 2013.

[6] M. Qin and J. Xu, “Improved pulse regulation control technique for switching DC–DC converters operating in DCM,” *IEEE Trans. Ind. Electron.*, Vol. 60, No. 5, pp. 1819-1830, May 2013.

[7] Z. Sun, K. W. R. Chew, H. Tang, and L. Siek, “Adaptive gate switching control for discontinuous conduction mode DC–DC converter,” *IEEE Trans. Power Electron.*, Vol. 29, No. 3, pp. 1311-1320, Mar. 2014.

[8] J. Sha, J. Xu, S. Zhong, S. Liu, and L. Xu, “Control pulse combination-based analysis of pulse train controlled DCM switching DC–DC converters,” *IEEE Trans. Ind. Electron.*, Vol. 62, No. 1, pp. 246-255, Jan. 2015.

[9] J. A. Abu Qahouq, “Control scheme for sensorless operation and detection of CCM and DCM operation modes in synchronous switching power converters,” *IEEE Trans. Power Electron.*, Vol. 25, No. 10, pp. 2489-2495, Oct. 2010.

[10] J. Morroni, L. Corradini, R. Zane, and D. Maksimovic, “Adaptive tuning of switched-mode power supplies operating in discontinuous and continuous conduction modes,” *IEEE Trans. Power Electron.*, Vol. 24, No. 11, pp. 2603-2611, Nov. 2009.

[11] J. A. Abu Qahouq, “Control scheme for sensorless operation and detection of CCM and DCM operation modes in synchronous switching power converters,” *IEEE Trans. Power Electron.*, Vol. 25, No. 10, pp. 2489-2495, Oct. 2010.

[12] A. D. Martin, J. R. Vazquez, and R. S. Herrera, “Adaptive backstepping control of a DC-DC converter in photovoltaic systems,” *EUROCON*, *2013 IEEE*, pp. 949-955, 2013.

[13] M. Salimi, J. Soltani, A. Zakipour, and V. Hajbani, “Two-loop adaptive and nonlinear control of the DC-DC boost converter in Discontinuous Conduction Mode,” *Power Electronics, Drive Systems and Technologies Conference (PEDSTC)*, 2013 4th, pp. 164-169, 2013.

[14] S. Oucheriah and L. Guo, “PWM-based adaptive sliding-mode control for boost DC–DC converters,” *IEEE Trans. Ind. Electron.*, Vol. 60, No. 8, pp. 3291-3294, Aug. 2013.

[15] H. El-Fadil and F. Giri, “Robust nonlinear adaptive control of multiphase synchronous buck power converters,” *Control Engineering Practice,* Vol. 17, No. 11, pp. 1245-1254, Nov. 2009.

[16] M. Salimi, J. Soltani, G. A. Markadeh, and N. R. Abjadi, “Indirect output voltage regulation of DC–DC buck/boost converter operating in continuous and discontinuous conduction modes using adaptive backstepping approach,” *IET Power Electron.*, Vol. 6, No. 4, pp. 732-741, Apr. 2013.

Mahdi Salimi was born in Ardabil, Iran, in 1979. He received his B.S. and M.S. degrees in Electrical Engineering from K.N.T University of Technology, Tehran, Iran, in 2000 and 2002, respectively, and his Ph.D. degree in Power Electronics from Science and Research Branch, Islamic Azad University, Tehran, Iran, in 2012. Since 2003, he has been with Islamic Azad University, where he is currently Assistant Professor at the Department of Electrical Engineering. His research interests include closed-loop control of power electronics converters, high gain DC–DC converters, grid-connected inverters, and renewable energy.

Adel Zakipour was born in Ardabil, Iran, in 1981. He received his B.S. and M.S. degrees in Electrical Engineering from Islamic Azad University, Ardabil, Iran, and Iran University of Science and Technology, Tehran, Iran, in 2002 and 2004, respectively. He is currently working toward his Ph. at K.N.T University of technology. Since 2005, he has been with Islamic Azad University. His research interests include power electronics and variable speed drive.